How to cite: *Angew. Chem. Int. Ed.* **2024**, *63*, e202404286
doi.org/10.1002/anie.202404286

VIP **Membrane Transport** *Very Important Paper*

Size and Polarizability of Boron Cluster Carriers Modulate Chaotropic Membrane Transport

Giulia Salluce, Yeray Folgar-Cameán, Andrea Barba-Bon, Ivana Nikšić-Franjić, Suzan El Anwar, Bohumír Grüner, Irene Lostalé-Seijo, Werner M. Nau,* and Javier Montenegro**

Abstract: Perhalogenated *closo*-borates represent a new class of membrane carriers. They owe this activity to their chaotropicity, which enables the transport of hydrophilic molecules across model membranes and into living cells. The transport efficiency of this new class of cluster carriers depends on a careful balance between their affinity to membranes and cargo, which varies with chaotropicity. However, the structure–activity parameters that define chaotropic transport remain to be elucidated. Here, we have studied the modulation of chaotropic transport by decoupling the halogen composition from the boron core size. The binding affinity between perhalogenated decaborate and dodecaborate clusters carriers was quantified with different hydrophilic model cargos, namely a neutral and a cationic peptide, phalloidin and $(KLAKLAK)_2$. The transport efficiency, membrane-lytic properties, and cellular toxicity, as obtained from different vesicle and cell assays, increased with the size and polarizability of the clusters. These results validate the chaotropic effect as the driving force behind the membrane transport propensity of boron clusters. This work advances our understanding of the structural features of boron cluster carriers and establishes the first set of rational design principles for chaotropic membrane transporters.

Introduction

The delivery of hydrophilic molecules across membranes by supramolecular association with superchaotropic boron clusters has been recently introduced.[1–4] Transport by the series of perhalogenated *closo*-dodecaborates follows a different mechanism from that of amphiphilic molecules, as it is driven by the chaotropic effect rather than the traditional amphiphilic activation.[5–12] In contrast to the classical hydrophobic effect, chaotropic membrane transport shows an enthalpy-driven signature.[5,13] In this context, *closo*-borates were one of the first ions identified as being superchaotropic,[6,14] i.e., their properties exceed those of the most chaotropic ions on the Hofmeister's series,[5,15] a characteristic they share with other large anions, such as COSANs,[3,16] polyoxometalates,[14,17–19] or chalcogenide clusters.[20]

The peculiar properties of superchaotropic clusters are related to strong dehydration effects and dispersion interactions of these large, charge-delocalized anions.[6,13,21–25] Due to their high boron content, bulky size, special 3D aromaticity,[26] and biocompatibility,[27] *closo*-borates have been developed as enabling chemical tools for biology and biomedicine.[28–32] Their biocompatibility and medicinal potential has been shown in boron neutron capture therapy, either as derivatives or tethered to tumor-targeted carriers, to deliver sufficient ^{10}B isotopes into cancer cells.[29,33,34] They can be conjugated to small molecules,[30,35] peptides,[36] and oligonucleotides.[37,38] Their affinity towards hydrophobic cavities,[6] polymers,[27] proteins,[39] or membranes[40,41] is reminiscent of that of amphiphilic molecules.[16,42] In our previous work,[1] by using dodecaborates with different substituents, we were able to infer the dependence of the transport activity on the cluster substitution. However, the physicochemical properties that control their potential transport across membranes, as well as their recently observed carrier behavior, have yet to be unfolded.

[*] Dr. G. Salluce, Y. Folgar-Cameán, Dr. I. Lostalé-Seijo, Prof. Dr. J. Montenegro
Centro Singular de Investigación en Química Biolóxica e Materiais Moleculares (CiQUS)
Departamento de Química Orgánica
Universidade de Santiago de Compostela, 15705, Santiago de Compostela Spain
E-mail: irene.lostale@usc.es
javier.montenegro@usc.es

Dr. A. Barba-Bon, Dr. I. Nikšić-Franjić, Prof. Dr. W. M. Nau
School of Science, Constructor University
Campus Ring 1, 28759 Bremen, Germany
E-mail: wnau@constructor.university

Dr. S. El Anwar, Dr. B. Grüner
Institute of Inorganic Chemistry, Czech Academy of Sciences, v.v.i. Hlavní 1001, CZ-250 68 Řež, Czech Republic

We now demonstrate that the size and polarizability of di-anionic borate cluster carriers are the fundamental parameters that govern chaotropic membrane transport, and not their chemical composition. We have selected the well-studied and most stable decaborate ($B_{10}X_{10}^{2-}$) and dodecaborate ($B_{12}X_{12}^{2-}$) families (X=H, Cl, Br, I) to decouple the effect of cluster size and polarizability from the nature of the halogen substituent (Figure 1). In comparison to the *closo*-dodecaborates ($B_{12}X_{12}^{2-}$), the smaller decaborates ($B_{10}X_{10}^{2-}$) do not show an icosahedral symmetry (I_h) of the molecular structure, presenting two types of boron atoms in the bicapped square antiprismatic arrangement (hexadecahedral, D_{4d} point group).[39,43,44] Decaborate clusters adopt a prolate ellipsoid rather than a spherical shape, with apical boron atoms formally only tetracoordinated to their neighbors, which leads to a partial localization of the charge in these sites.[39,44] This geometrical feature renders them more susceptible to electrophilic reactions and interactions with water molecules.[32,45,46] Both $B_{10}X_{10}^{2-}$ and $B_{12}X_{12}^{2-}$ share the two negative charges and the low charge density typical of superchaotropic anions,[21,22] which allows a direct comparison to be made between them. Thus, we compare herein their affinity to two model hydrophilic peptide cargos, and we carefully study their transport performance in vesicles and living cells. The objective of this study is to advance in our understanding of the underlying principles behind the transport activity of these nonclassical anionic carriers and to obtain structure–activity relationships for the rational design of chaotropic transporters.

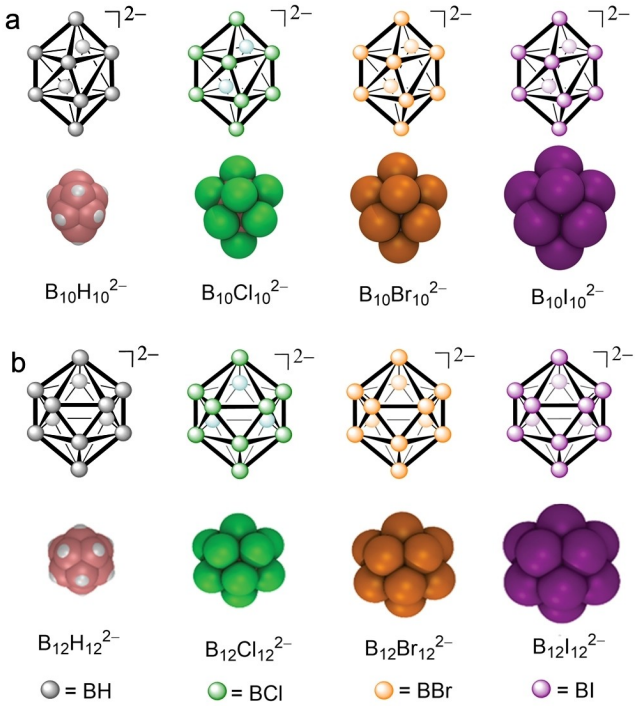

Figure 1. a) Decaborate and b) dodecaborate cluster series (chemical structures, top, and molecular models, bottom).

Results and Discussion

Chaotrope-Mediated Transport through Model Membranes

The ability of *closo*-deca- and dodecaborates to act as membrane carriers was first evaluated in large unilamellar vesicles loaded with the 8-hydroxypyrene-1,3,6-trisulfonate/*p*-xylene-bis-pyridinium (HPTS/DPX) reporter pair (Figure 2a).[47] In this particular assay, the negatively charged dye (HPTS) is co-encapsulated with a cationic quencher (DPX) ensuring efficient fluorescence quenching. However, in the presence of a suitable carrier, the impermeable cargo can move through the lipid bilayer (step *iii* in Figure 2a) into the liposomal phase. Due to the reversibility of the binding (see below), the cluster·cargo complex can dissociate (step *iv*), granting "free" cluster to interact with the positively charged quencher (step *v*, see also Figure S6). The resulting complex can shuttle back out through the lipid membrane (step *vi*), yielding an increase in HPTS fluorescence, which signals successful membrane transport in the microheterogeneous system.

Two hydrophilic functional peptides were selected as model cargos (Figure S2): *i*) phalloidin as a neutral zwitterionic cargo and *ii*) $(KLAKLAK)_2$ as a cationic pro-apoptotic peptide. The opening for chaotrope-mediated transport is the association between the boron cluster and the cargo (step *i* in Figure 2a). Therefore, the interaction between the deca- and dodecaborates and the peptides was studied by isothermal titration calorimetry (ITC, Figure 2b, Table 1, Figures S3–S5, and Table S1).

No significant heat was observed for the parent hydrogenated derivatives ($B_{10}H_{10}^{2-}$ and $B_{12}H_{12}^{2-}$), indicating a weak interaction with the peptides due to their lower chaotropicity. However, all perhalogenated clusters showed sufficiently strong interactions (on the order of $10^4\ M^{-1}$) that allow the carrier·cargo complexes to form, to associate with the lipid bilayer (step *ii* in Figure 2a), and to shuttle through the membrane (step *iii*). In addition, the micromolar affinity allows the reversible release of the peptide into the interior of the vesicles. The binding affinity was in most cases enthalpically driven, with a negative entropic component, in line with the chaotropic effect[5] as driving force for the supramolecular interaction. The binding increased with cluster size: for example, the affinity of dodecaborates was higher than that of the homologous decaborates and, when fixing the boron cluster, the affinity increased with the size of the halogen substituent. This observation points to a general correlation between the chaotropicity of the clusters and their generic affinity to biomolecules, which is supported by previous literature trends for albumins[39] or cyclodextrins[6] as interaction partners. Lastly, comparison of the calorimetry data between the two peptide cargos indicated that, in general, the cluster binding constant was significantly higher towards the cationic amphiphilic $(KLAKLAK)_2$ than the neutral (uncharged) hydrophilic phalloidin cyclic peptide (Table 1, Figure S15). We attribute the stronger binding of cationic peptides to additional electrostatic (charge-charge) interactions with all di-anionic clusters. The less negative binding entropy terms for the cationic

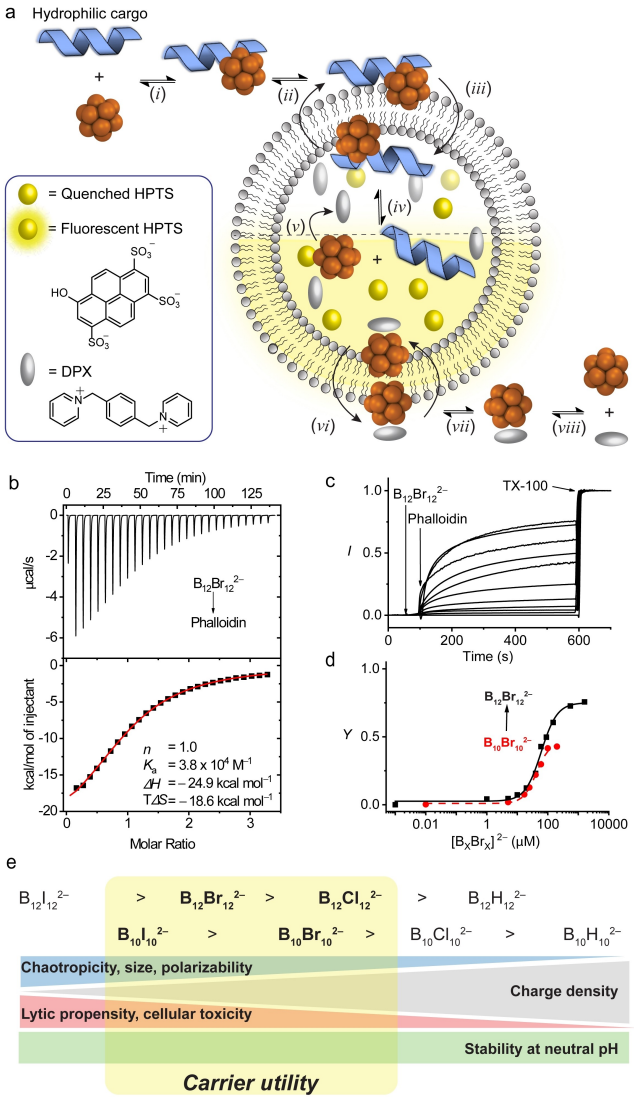

Figure 2. a) Schematic representation of the transport mechanism activated by boron clusters, signaled by the HPTS/DPX assay, along with the chemical structures of the fluorescent dye (HPTS) and quencher (DPX). b) Representative microcalorimetric titration in water: thermogram (top) for the sequential injection of $B_{12}Br_{12}^{2-}$ (1 mM) into phalloidin (90 μM) and corresponding reaction heats from the integration of the calorimetric traces (bottom). c) Representative changes in HPTS emission in EYPC⊃HPTS/DPX vesicles as a function of time upon addition of increasing concentrations of $B_{12}Br_{12}^{2-}$ (0–1600 μM, from bottom to top), phalloidin (20 μM), and TX-100 for calibration. d) Dose-response curves for phalloidin transport by the brominated derivatives, $B_{10}Br_{10}^{2-}$ and $B_{12}Br_{12}^{2-}$. e) Organization of the evaluated *closo*-borates according to their chaotropicity, charge density, and expected membrane lytic properties; the window of carrier utility is highlighted in yellow.

peptides compared to phalloidin support this interpretation (Table S1).[48]

Once we had confirmed that the binding is governed by the chaotropic effect, we studied the transport of the selected hydrophilic peptides across model membranes. In the time-resolved fluorescence experiments, the fluorescence intensity of HPTS is monitored during the addition of the boron cluster (as carrier, $t = 50$ s) and the impermeable peptide (as cargo, $t = 100$ s). A surfactant (Triton X-100, TX-100) is added at the end of the experiment ($t = 600$ s) to release all content and allow data normalization (Figure 2c). Both iodinated derivatives ($B_{10}I_{10}^{2-}$ and $B_{12}I_{12}^{2-}$) showed a steep increase in fluorescence when they were added to the vesicles (even without cargo) indicating membrane disruption, which was also confirmed by dynamic light scattering (DLS) measurements (Figures S7–S12). This lytic activity can be related to the highest chaotropicity of these largest clusters. Nevertheless, addition of the other clusters alone did not afford any significant increase of the fluorescence in the absence of cargo, confirming the lack of any permanent membrane damage and of the formation of any stable membrane pore for these clusters ($B_xH_x^{2-}$, $B_xCl_x^{2-}$, $B_xBr_x^{2-}$, Figures S7–S12). DLS experiments of vesicle suspensions further confirmed the integrity of the lipid bilayer in the presence of the non-iodinated cluster carriers.

When cargo was added, the non-halogenated parent ions ($B_{10}H_{10}^{2-}$ and $B_{12}H_{12}^{2-}$), which are the smallest and, therefore, the least chaotropic clusters, did not show strong transport activity, although an incipient transport of $(KLAKLAK)_2$ was spotted at high $B_{12}H_{12}^{2-}$ concentrations (Figure S10). All chlorinated and brominated clusters, being intermediate in size and chaotropicity, showed transport after cargo addition without membrane disruption (Figures S7–S12). To quantify the transport ability of the active clusters, the normalized fluorescence response was plotted versus the cluster concentration to afford dose-response curves (Figure 2d, Figures S7–S12) and subsequently analyzed by Hill analysis. This analysis provided the characteristic membrane transport parameters: Y_{max}, the maximal activity; and EC_{50}, the cluster concentration required to reach 50 % of maximal activity; E_a, the activator efficiency,[49] was calculated by involving the previous two parameters (see Methods) to compare different membrane carriers (Table 1, Table S2). The observed trend is that, independent of the evaluated peptide cargo, dodecaborates show higher transport activity than decaborates. This transport scale can be understood in terms of the cluster size (and chaotropicity), where the smallest derivatives ($B_xH_x^{2-}$) lack chaotropicity to activate transport of impermeable cargos and the largest clusters ($B_xI_x^{2-}$) can induce membrane lysis in vesicles. Based on their chaotropicity, one would expect the brominated clusters to have a higher transport activity than their chlorinated homologs, but $B_{12}Cl_{12}^{2-}$ with phalloidin as cargo presents an exception here, as it is remarkably more active than $B_{12}Br_{12}^{2-}$ (Table 1, Figure S15). This observation could be related to the macrocyclic structure of the phalloidin ring which may introduce an additional size selectivity, similar to that observed in the binding of the clusters to cyclodextrins.[6,24]

Experiments in Living Cells

To transfer the findings from vesicles to cellular membranes, the toxicity of the clusters was evaluated first by MTT assay

Table 1: Binding affinities and membrane transport efficiencies of *closo*-borate clusters towards the selected cargo molecules, and half-maximum inhibitory concentrations (IC_{50}) as an indicator of their cellular toxicity.

Cluster	Phalloidin (789 g/mol; neutral)		(KLAKLAK)$_2$ (1,522 g/mol; charge +7)		IC_{50}[a]
	$K_a/10^4$ (M^{-1}) [b]	E_a[c]	$K_a/10^4$ (M^{-1}) [b]	E_a	(μM)
$B_{10}H_{10}^{2-}$ [d]	n.h.[e]	n.a.[f]	n.h.	n.a.	>2000
$B_{10}Cl_{10}^{2-}$ [g]	2.0	2.6	0.3, 1.5[h]	8.1	>2000
$B_{10}Br_{10}^{2-}$ [g]	2.2	3.1	1.9, 78.2[h]	10.8	>2000
$B_{10}I_{10}^{2-}$ [g]	6.5	d.l.[i]	96.7	d.l.	156
$B_{12}H_{12}^{2-}$ [d]	n.h.	n.a.	n.h.	0.3	>2000
$B_{12}Cl_{12}^{2-}$ [d]	3.5	8.6	0.1, 1.3[h]	10.6	>2000
$B_{12}Br_{12}^{2-}$ [d]	3.8	4.3	2.2, 81.2[h]	11.9	987
$B_{12}I_{12}^{2-}$ [d]	7.4	d.l.	219.0	d.l.	64

[a] Data obtained by MTT assay after 3 h incubation of clusters with HeLa cells at concentrations up to 2 mM. Each Abs_{570} value was normalized to the mean value of untreated control, and employed to calculate the IC_{50} by fitting to the Hill equation (see SI). [b] Obtained by ITC (see SI). [c] Membrane transport efficiency calculated in EYPC vesicles (13 μM phospholipids) with 20 μM cargo, see Supporting Information for details. [d] Used as sodium salt. [e] n.h. = no reaction heat. [f] n.a. = no detectable activity in the vesicles experiments. [g] Used as cesium salt; analogous experiments with sodium and cesium salts of $B_{12}Cl_{12}^{2-}$ and $B_{12}Br_{12}^{2-}$ confirmed that the counter cation does not significantly affect the transport activity at the chosen concentrations. [h] Two-binding-sites model was used to fit the data. [i] d.l. = dye leakage, no determination possible.

in HeLa cells, affording the IC_{50} of the clusters (Table 1, Figure S13). In line with the vesicle experiments, both iodinated clusters showed higher toxicity while the (smallest) parent clusters did not show significant cell death, with $IC_{50} > 2$ mM. Chlorinated and brominated clusters showed good cell compatibility, where only $B_{12}Br_{12}^{2-}$ showed moderate toxicity with $IC_{50} \sim 1$ mM, which is orders of magnitude higher than the concentrations required for successful intracellular delivery (see below).

Phalloidin is a membrane-impermeable rigid bicyclic heptapeptide (Figure S2) commonly employed in cell biology to label F-actin of the cytoskeleton,[50] and constitutes an ideal neutral (uncharged) model to monitor membrane translocation of a functional cargo[1,51,52] (Figure 3). Confocal microscopy of living HeLa cells with the fluorescent derivative TRITC (tetramethylrhodamine) provided a qualitative outcome of internalization of the fluorescent cargo with the eight clusters of this study (Figure 3a–h), which was further quantified by flow cytometry measurements (Figure 3i).

In the decaborate series ($B_{10}X_{10}^{2-}$), a systematic trend towards stronger F-actin staining (Figure 3a–d) and increased cytosolic phalloidin delivery (Figure 3i) with increasing chaotropicity of the clusters was observed, in the order $B_{10}H_{10}^{2-} < B_{10}Cl_{10}^{2-} < B_{10}Br_{10}^{2-} < B_{10}I_{10}^{2-}$. In the dodecaborate series ($B_{12}X_{12}^{2-}$), the same trend with substituents applied (Figure 3e–h)[1] but the morphology of cells incubated with $B_{12}I_{12}^{2-}$ was severely compromised, which also led to a decrease in transport activity as detected by flow cytometry (Figure 3i).

The cross-comparison of the two series (Figure 3) showed that both hydrogenated clusters ($B_{12}H_{12}^{2-}$ and $B_{10}H_{10}^{2-}$) did not transport phalloidin, even at the highest tested concentrations. The higher activity of the larger homologous dodecaborates, $B_{12}Cl_{12}^{2-} > B_{10}Cl_{10}^{2-}$ and $B_{12}Br_{12}^{2-} > B_{10}Br_{10}^{2-}$, fully aligns with their higher chaotropicity. Interestingly, the activity of $B_{12}Cl_{12}^{2-}$ exceeded that of $B_{10}Br_{10}^{2-}$ (verified by flow cytometry, Figure 3i), despite the larger size of the latter, matching our previous observations on K_a and vesicle transport (Table 1 and Figure S15). However, the largest cluster ($B_{12}I_{12}^{2-}$) displayed cytotoxic effects, which became also apparent for the smaller $B_{10}I_{10}^{2-}$ at the higher concentrations (Figure 3i, S14). Consequently, the brominated dodecaborate ($B_{12}Br_{12}^{2-}$) strikes the best balance as it exhibits excellent transport capacity while maintaining the cellular morphology across the entire tested concentration range.

This result showcases how the size of the boron cluster core modulates the effect of halogen substitution in chaotropic membrane transport. While the iodinated dodecaborate cluster showed strong toxicity and aggregation with the phalloidin cargo, the smaller decaborate iodinated analogue showed an excellent delivery profile and actin labeling at low carrier concentration (Figure 3). As an additional corollary, these results confirm that it is not the chemical nature of the B-Halogen bonds *per se* which causes toxicity, but rather the generic size of the cluster.

To validate the confocal microscopy studies, the uptake of labeled phalloidin in HeLa cells incubated with the clusters was quantified by flow cytometry (Figure 3i, S14). In all cases, the outcome was consistent with what we observed by microscopy. The increase in size of the substituents (H < Cl < Br < I) was associated with a gradual increase of the transport capacity within each decaborate or dodecaborate series. This transport efficiency tends to decrease as the combination of concentration and chaotropicity reaches a toxic threshold. The smallest and least chaotropic boron clusters—$B_{10}H_{10}^{2-}$, $B_{12}H_{12}^{2-}$, and $B_{10}Cl_{10}^{2-}$—were confirmed as inactive carriers for intracellular transport (Figure 3i, bars). Interestingly, $B_{10}I_{10}^{2-}$ and $B_{12}Br_{12}^{2-}$, which have comparable size, showed almost identical phalloidin-TRITC internalization at the lowest concentration tested but, at higher concentrations, the former displayed slightly higher toxicity.

The $(KLAKLAK)_2$[55] peptide was subsequently employed to investigate the delivery of a bioactive cargo in

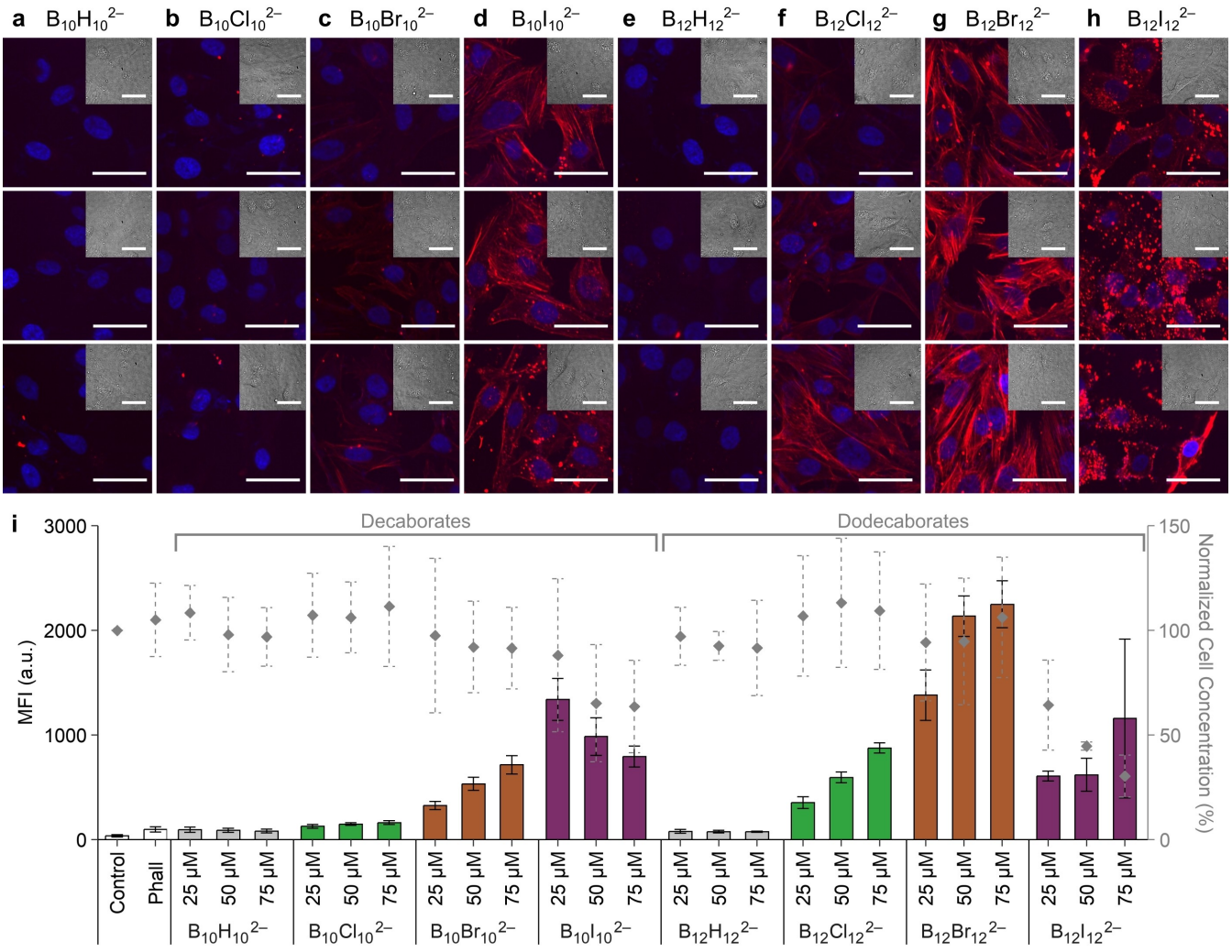

Figure 3. a–h) Confocal microscopy images of cluster-assisted phalloidin-TRITC transport into living HeLa cells. Cells were incubated with 2.5 µM phalloidin-TRITC (red) in the presence of different concentrations of globular deca- and dodecaborate clusters (25, 50, and 75 µM; first, second, and third row, respectively) in HEPES-Krebs-Ringer buffer (HKR; see SI) for 3 h, subsequently stained with the nuclear stain Hoechst (blue), washed with HKR buffer, and imaged by confocal fluorescence microscopy; bright-field images are shown in the insets. Scale bars: 50 µm. i) Flow cytometry quantification of cluster-assisted phalloidin-TRITC transport into HeLa cells. Cells were incubated with phalloidin-TRITC and different concentrations of globular deca- and dodecaborates as in a–h, and subsequently washed with PBS, trypsinized, and analyzed by flow cytometry. Bars represent the mean of the median fluorescence intensity (MFI, left axis) of phalloidin-TRITC; grey diamonds represent the cell concentrations normalized on untreated cells (right axis). Error bars represent SD of three biological replicates, each one with three technical replicates. Note that, although the cytosolic delivery of phalloidin may lead to toxicity and inhibition of cell proliferation,[53,54] this is unlikely to manifest itself in such a short period of time and the reduction in the number of cells with normal morphology observed by flow cytometry can be used as measure of the cytotoxicity of each cluster. See Figure S14 for the associated histograms.

cells. Once delivered into the cytosol, $(KLAKLAK)_2$ causes mitochondria permeabilization and triggers cell apoptosis.[56,57] Thus, the $(KLAKLAK)_2$ peptide was incubated with cells in the presence of different concentrations of clusters and the cell viability was determined by MTT assay. The cluster-enhanced cytosolic delivery of $(KLAKLAK)_2$ can thus be quantified by measuring the decrease in cell viability in samples co-incubated with the clusters, as compared to controls treated with the peptide or the clusters alone.

As in the case of phalloidin-TRITC, the extent of $(KLAKLAK)_2$ internalization correlated with the size and chaotropicity of each cluster and with the cluster concentration (Figure 4). As expected, the two hydrogenated clusters ($B_{10}H_{10}^{2-}$ and $B_{12}H_{12}^{2-}$) were consistently inactive in $(KLAKLAK)_2$ delivery. The chlorinated and the brominated decaborates were only slightly active at the highest concentration tested (100 µM). The brominated dodecaborate ($B_{12}Br_{12}^{2-}$) showed good transport efficiency for $(KLAKLAK)_2$, as evidenced by the difference in cell viability between the samples incubated with and without the toxic peptide at cluster concentrations above 50 µM. However, while the iodinated dodecaborate ($B_{12}I_{12}^{2-}$) was highly toxic and showed a rapid decrease in viability even in the absence of the pro-apoptotic peptide, the decaborate analogue ($B_{10}I_{10}^{2-}$) showed an optimal intracellular delivery

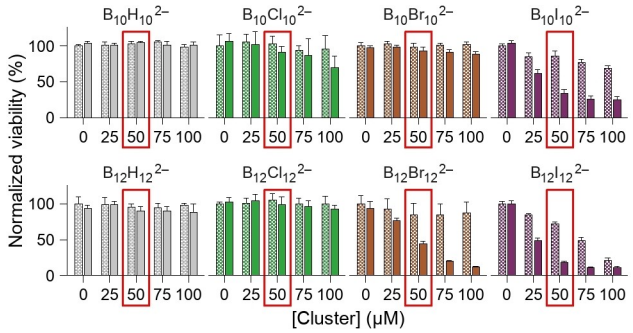

Figure 4. Cluster-mediated internalization of $(KLAKLAK)_2$ peptide. HeLa cells were incubated with 0 (left patterned bars) or 50 μM (right solid bars) of the pro-apoptotic peptide in the absence or presence of the indicated concentrations of globular clusters in HKR buffer for 3 h, replaced with fresh medium for 24 h. Thereafter, viability was determined by MTT assay. Bars represent viability normalized to untreated cells, error bars represent SD of five technical replicates. Red boxes highlight the 50 μM concentrations discussed in the text.

Table 2: Molecular volumes and polarizabilities of boron clusters.

	V_{exp} (Å^3) [a]	V_{calc} (Å^3) [b]	α_{exp} (Å^3) [c]	α_{calc} (Å^3) [b]
$B_{10}H_{10}^{2-}$	125	130	18.9	23.3
$B_{12}H_{12}^{2-}$	145	151	22.0	25.1
$B_{10}Cl_{10}^{2-}$	279	282	36.9	40.6
$B_{12}Cl_{12}^{2-}$	331	333	44.0	46.2
$B_{10}Br_{10}^{2-}$	352	356	48.7	52.8
$B_{12}Br_{12}^{2-}$	419	423	57.1	60.2
$B_{10}I_{10}^{2-}$	432	436	(60.5) [d]	65.3
$B_{12}I_{12}^{2-}$	515	521	(70.4) [d]	76.0

[a] From crystal structures (CCDC [COD] codes ANUDEV, ACERIJ, BIPVOO, HEGVOH, [1536635], AMENUE, CAGJAW, TILTAN). [b] From DFT-calculated gas-phase structures (B3LYP–D3/6–311+G(2d,p) level of theory, LANL2DZ ECP for iodine; note the excellent correlation: $V_{exp}=0.989\times V_{calc}$, $n=6$, $r^2=1.000$. [c] From refractive index measurements in dimethyl sulfoxide solution, see ref.[21,22]. [d] Values extrapolated from a linear correlation, $\alpha_{exp}=0.927\times\alpha_{calc}$, $n=6$, $r^2=0.997$.

of the $(KLAKLAK)_2$ peptide with little toxicity, in the low concentration regime ($\leq$50 μM). Therefore, $B_{10}I_{10}^{2-}$ is as active as $B_{12}Br_{12}^{2-}$ at the intermediate concentration of 50 μM.

At higher concentrations, the toxicity of the iodinated decaborate increased relatively more steeply than for the brominated dodecaborate ($B_{12}Br_{12}^{2-}$), due to the higher chaotropicity of $B_{10}I_{10}^{2-}$, but at a considerably lower rate than its $B_{12}I_{12}^{2-}$ counterpart. These results confirm the key role of cluster core size in modulating the biological performance of chaotropic cluster carriers in terms of delivery efficiency and cellular viability (Figure 4). The type of halogen determines the cluster activity nonspecifically—through its influence on the cluster size—and not specifically—through the nature of its intramolecular bonds or intermolecular bonding.

The affinity of boron clusters to membranes and peptides has been attributed conceptually to the chaotropic effect and thermochemically to enthalpic dehydration effects and dispersion interactions, which are governed by the size and polarizability of the clusters, respectively.[5,6,17] Chaotropicity of anions has been directly related, unless there are differences in net charge or dipole moment,[3,17,58,59] to their polarizability.[60–63] To the extent that also membrane transport is governed by the chaotropicity of the cluster carriers, it should correlate with these structural and physicochemical molecular parameters. The volumes of the investigated clusters (from calculated geometries or solid-state crystallographic structures) and experimental polarizabilities (from refractive index measurements) are shown in Table 2. Note that the polarizability of decaborates is significantly lower than that of their $B_{12}X_{12}^{2-}$ counterparts,[21,22] such that the two homologous series interdigitate perfectly, allowing a large and systematic variation in molecular volumes (from 125–515 Å^3) as well as polarizabilities (19–70 Å^3), by about a factor of 4. As can be seen from Figures 4 and 5, the membrane transport activity of boron clusters with $(KLAKLAK)_2$ peptide as cargo increased indeed with their polarizability ($\leq$ 50 μM) until a turning point at too high cluster concentration when the most chaotropic iodinated boron clusters became toxic (>50 μM). When molecular size (volume) instead of polarizability is used for correlation, the bioactivity trend of the boron clusters remains the same. This is expected because there is a linear correlation between volume and polarizability ($V_{exp}=7.32\times\alpha_{exp}$, $n=6$, $r^2=0.995$), which renders the dissection of dehydration versus dispersion effects in general difficult.[64] In fact, it has been proposed that several aspects of the peculiar behavior of superchaotropic anions can be accounted for by considering their size alone.[17,25] Be this as it may, our study provides one of the rare cases where biological activity in living cells or organisms can be directly correlated with a fundamental molecular property of the ionic additives.[63,65]

Besides the obvious trends with size and polarizability, some additional conclusions can be drawn. First, there is no absolute threshold at which a cluster becomes transport-active, but it depends on the cargo (Figure 5 and S15). For example, the minimum threshold of polarizability that allows transport activation in cells is located around 40 Å^3 for phalloidin, in between $B_{10}Cl_{10}^{2-}$ and $B_{12}Cl_{12}^{2-}$, but around 55 Å^3 for $(KLAKLAK)_2$, in between $B_{10}Br_{10}^{2-}$ and $B_{12}Br_{12}^{2-}$. Second, the more polarizable (larger, more chaotropic) clusters require lower concentrations to carry out the intracellular transport. A clear trend of increased amount of cargo transported with higher polarizability is observed (Figures 3, 4, S15), that was offset by the toxicity of some cluster/concentration combinations (e.g., the iodinated dodecaborate in Figure 3i shows lower phalloidin transport than other clusters with lower polarizability). As a counteracting effect, there is also a clear dependence of toxicity on polarizability, expressed by the IC_{50} values (Table 1, Figure S13, S15), as well as by the transport activities (Figure 5 and Figure S15). It should be noted that the trends for dianionic borate clusters may not be directly extrapolated to any other superchaotropic anions, such as cobalt bisdicarbollides[3] or polyoxometalates,[18] as their net charge and intrinsic cargo specificity can differ.

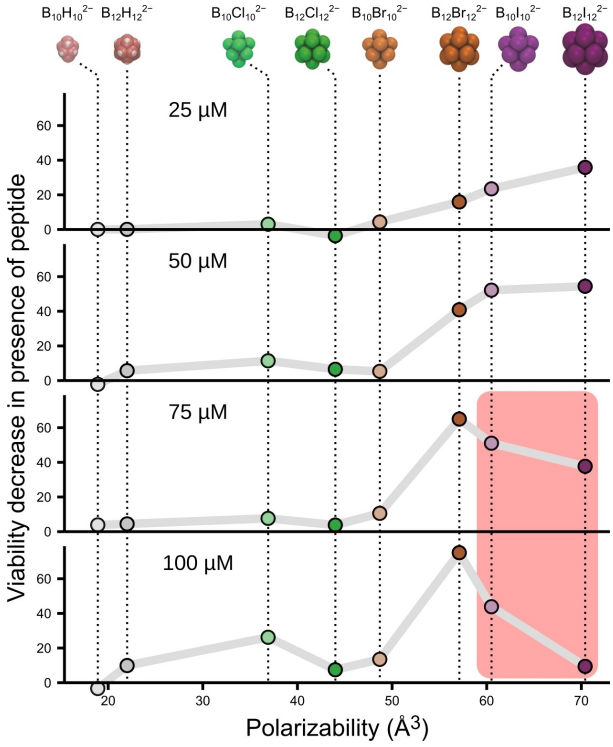

Figure 5. Relationship between cluster polarizability and $(KLAKLAK)_2$ transport, as measured through its cytotoxicity. Data calculated from the difference in viability in the presence of the indicated concentrations of cluster (25, 50, 75, 100 µM) and 50 µM $(KLAKLAK)_2$ with respect to the viability after incubation with the indicated concentration of cluster alone; see Figure 4. In the red highlighted inset, the intrinsic toxicity of the iodinated clusters offsets peptide delivery, thus showing a lower viability decrease when compared to clusters with lower polarizability.

Conclusions

Our study of two *closo*-borate cluster families with 10 and 12 boron atoms and their perfunctionalization with different monovalent atoms (H, Cl, Br, I) has allowed a systematic variation of their physicochemical properties (chaotropicity, size, polarizability, charge density) over a large range and to correlate them with relevant activity parameters (affinity to peptides, membrane transport efficiency, membrane lytic propensity, cellular uptake, and cellular toxicity). This afforded the first clear structure–activity relationships for this new class of chaotropic membrane carriers (Figure 2e). As a rule, high chaotropicity, cluster size, and cluster polarizability results in higher affinity constants with the transported cargo molecules, in more efficient membrane transport in vesicles and cells, but also in higher membranelytic propensity and cellular toxicity, likely due to too strong interactions with the biomembranes. Accordingly, there is a window of carrier utility, which is reached for an intermediary cluster size, in between $B_{12}Cl_{12}^{2-}$ and $B_{10}I_{10}^{2-}$. The most chaotropic cluster ($B_{12}I_{12}^{2-}$) is less useful because it causes membrane damage, while the smallest cluster ($B_{10}H_{10}^{2-}$) is the least active one because of its lowest chaotropicity (Figure 2e). Mechanistically, a higher chaotropicity is related to a larger cluster size, lower charge density, and increased polarizability of the clusters, which accounts for the higher affinity to biological components, both peptides and membranes, on account of favorable dehydration effects and dispersion interactions in aqueous solution.[5,6,13,27,39–41] This work serves as a blueprint for the design and implementation of chaotropic clusters and their formulations with potential membrane transporting capabilities. For instance, as we have observed that boron clusters with lower chaotropicity (polarizability, size) require higher concentrations for transport and *vice versa*, the cluster type may be selected according to the required concentration of active molecule that has to be delivered into cells. In addition, these results indicate that adjusting the polarizability and the size of cluster carriers is key to balance an efficient membrane transport versus membrane disruption. Since the molecular polarizabilities—in contrast to the chaotropicity of anions—can be experimentally determined, this parameter may serve as a predictor for carrier activity and toxicity of superchaotropic ions of the same net charge.

Acknowledgments

J.M. thanks the Spanish AEI (PCI2019-103400, PID2020-117143RB-I00), the Xunta de Galicia (Centro singular de investigación de Galicia accreditation 2019–2022, ED431G 2019/03, ED431F 2023/12, the Oportunius Program (GAIN)), Fundación la Caixa (TROPIC, HR23-00221), and the European Regional Development Fund (ERDF). G.S. and Y.F.-C. thank AEI for their predoctoral fellowships (PRE2018-085973; FPU21/04747); G.S. thanks Xunta de Galicia for her postdoctoral contract (ED481B-2023-123). A.B.-B. and W.M.N. thank the Deutsche Forschungsgemeinschaft (DFG) for financial support through projects NA-868/14, NA-868/15 and NA-868/17; calculations were performed on a compute cluster funded by the DFG through project INST 676/7-1 FUGG. B.G. acknowledges financial support by the Czech Science Foundation through project No. 2114409S.

Conflict of Interest

The authors declare no conflict of interest.

Data Availability Statement

The data that support the findings of this study are available from the corresponding author upon reasonable request.

Keywords: Boron · Cluster compounds · Peptide delivery · Membranes · Vesicles

[1] A. Barba-Bon, G. Salluce, I. Lostalé-Seijo, K. I. Assaf, A. Hennig, J. Montenegro, W. M. Nau, *Nature* **2022**, *603*, 637–642.
[2] X. Hu, D. Guo, *Angew. Chem. Int. Ed.* **2022**, *61*, e202204979.

[3] Y. Chen, A. Barba-Bon, B. Grüner, M. Winterhalter, M. A. Aksoyoglu, S. Pangeni, M. Ashjari, K. Brix, G. Salluce, Y. Folgar-Cameán, J. Montenegro, W. M. Nau, *J. Am. Chem. Soc.* **2023**, *145*, 13089–13098.

[4] Y. Hirai, Y. Makita, J. Asaoka, Y. Aoyagi, A. Nomoto, H. Okamura, S. Fujiwara, *ACS Omega* **2023**, *8*, 35321–35327.

[5] K. I. Assaf, W. M. Nau, *Angew. Chem. Int. Ed.* **2018**, *57*, 13968–13981.

[6] K. I. Assaf, M. S. Ural, F. Pan, T. Georgiev, S. Simova, K. Rissanen, D. Gabel, W. M. Nau, *Angew. Chem. Int. Ed.* **2015**, *54*, 6852–6856.

[7] I. Lostalé-Seijo, J. Montenegro, *Nat. Chem. Rev.* **2018**, *2*, 258–277.

[8] I. Lostalé-Seijo, I. Louzao, M. Juanes, J. Montenegro, *Chem. Sci.* **2017**, *8*, 7923–7931.

[9] L. E. Bickerton, T. G. Johnson, A. Kerckhoffs, M. J. Langton, *Chem. Sci.* **2021**, *12*, 11252–11274.

[10] G. Gasparini, E.-K. Bang, J. Montenegro, S. Matile, *Chem. Commun.* **2015**, *51*, 10389–10402.

[11] S. Cavalli, F. Albericio, A. Kros, *Chem. Soc. Rev.* **2010**, *39*, 241–263.

[12] S. A. Bode, I. C. Kruis, H. P. J. H. M. Adams, W. C. Boelens, G. J. M. Pruijn, J. C. M. van Hest, D. W. P. M. Löwik, *ChemBioChem* **2017**, *18*, 185–188.

[13] K. Karki, D. Gabel, D. Roccatano, *Inorg. Chem.* **2012**, *51*, 4894–4896.

[14] B. Naskar, O. Diat, V. Nardello-Rataj, P. Bauduin, *J. Phys. Chem. C* **2015**, *119*, 20985–20992.

[15] F. Hofmeister, *Arch. für Exp. Pathol. und Pharmakologie* **1888**, *24*, 247–260.

[16] R. Fernandez-Alvarez, V. Ďorďovič, M. Uchman, P. Matějíček, *Langmuir* **2018**, *34*, 3541–3554.

[17] T. Buchecker, P. Schmid, S. Renaudineau, O. Diat, A. Proust, A. Pfitzner, P. Bauduin, *Chem. Commun.* **2018**, *54*, 1833–1836.

[18] A. Barba-Bon, N. I. Gumerova, E. Tanuhadi, M. Ashjari, Y. Chen, A. Rompel, W. M. Nau, *Adv. Mater.* **2024**, *36*, 2309219.

[19] M. Hohenschutz, P. Bauduin, C. G. Lopez, B. Förster, W. Richtering, *Angew. Chem. Int. Ed.* **2023**, *62*, e202210208.

[20] A. A. Ivanov, C. Falaise, P. A. Abramov, M. A. Shestopalov, K. Kirakci, K. Lang, M. A. Moussawi, M. N. Sokolov, N. G. Naumov, S. Floquet, D. Landy, M. Haouas, K. A. Brylev, Y. V. Mironov, Y. Molard, S. Cordier, E. Cadot, *Chem. A Eur. J.* **2018**, *24*, 13467–13478.

[21] A. Kaczmarczyk, G. B. Kolski, *J. Phys. Chem.* **1964**, *68*, 1227–1229.

[22] A. Kaczmarczyk, G. B. Kolski, *Inorg. Chem.* **1965**, *4*, 665–671.

[23] K. I. Assaf, J. Holub, E. Bernhardt, J. M. Oliva-Enrich, M. I. Fernández Pérez, M. Canle, J. A. Santaballa, J. Fanfrlík, D. Hnyk, W. M. Nau, *ChemPhysChem* **2020**, *21*, 971–976.

[24] K. I. Assaf, W. M. Nau, *Org. Biomol. Chem.* **2023**, *21*, 6636–6651.

[25] P. Dullinger, D. Horinek, *J. Am. Chem. Soc.* **2023**, *145*, 24922–24930.

[26] J. Poater, C. Viñas, I. Bennour, S. Escayola, M. Solà, F. Teixidor, *J. Am. Chem. Soc.* **2020**, *142*, 9396–9407.

[27] N. A. Bernier, J. Teh, D. Reichel, J. L. Zahorsky-Reeves, J. M. Perez, A. M. Spokoyny, *Langmuir* **2021**, *37*, 14500–14508.

[28] E. Hey-Hawkins, C. Viñas Teixidor, *Boron-Based Compounds: Potential and Emerging Applications in Medicine*, Wiley, **2018**.

[29] J. Cebula, K. Fink, J. Boratyński, T. M. Goszczyński, *Coord. Chem. Rev.* **2023**, *477*, 214940.

[30] V. V. Avdeeva, T. M. Garaev, E. A. Malinina, K. Y. Zhizhin, N. T. Kuznetsov, *Russ. J. Inorg. Chem.* **2022**, *67*, 28–47.

[31] Z. J. Leśnikowski, *J. Med. Chem.* **2016**, *59*, 7738–7758.

[32] J. C. Axtell, L. M. A. Saleh, E. A. Qian, A. I. Wixtrom, A. M. Spokoyny, *Inorg. Chem.* **2018**, *57*, 2333–2350.

[33] A. G. Beck-Sickinger, D. P. Becker, O. Chepurna, B. Das, S. Flieger, E. Hey-Hawkins, N. Hosmane, S. S. Jalisatgi, H. Nakamura, R. Patil, M. da G H Vicente, C. Viñas, *Cancer Biother. Radiopharm.* **2023**, *38*, 160–172.

[34] D. Dziura, S. Tabbassum, A. MacNeil, D. D. Maharaj, R. Laxdal, O. Kester, M. Pan, H. Kumada, D. Marquardt, *Can. J. Phys.* **2023**, *101*, 363–372.

[35] Y. Wang, A. M. Spokoyny, *ACS Cent. Sci.* **2022**, *8*, 309–311.

[36] K. Fink, K. Kobak, M. Kasztura, J. Boratyński, T. M. Goszczyński, *Bioconjugate Chem.* **2018**, *29*, 3509–3515.

[37] K. Ebenryter-Olbińska, D. Kaniowski, M. Sobczak, B. A. Wojtczak, S. Janczak, E. Wielgus, B. Nawrot, Z. J. Leśnikowski, *Chem. A Eur. J.* **2017**, *23*, 16535–16546.

[38] D. Kaniowski, K. Kulik, J. Suwara, K. Ebenryter-Olbińska, B. Nawrot, *Int. J. Mol. Sci.* **2022**, *23*, 12190.

[39] M. V. Kuperman, M. Y. Losytskyy, A. Y. Bykov, S. M. Yarmoluk, K. Y. Zhizhin, N. T. Kuznetsov, O. A. Varzatskii, E. Gumienna-Kontecka, V. B. Kovalska, *J. Mol. Struct.* **2017**, *1141*, 75–80.

[40] D. Awad, M. Bartok, F. Mostaghimi, I. Schrader, N. Sudumbrekar, T. Schaffran, C. Jenne, J. Eriksson, M. Winterhalter, J. Fritz, K. Edwards, D. Gabel, *ChemPlusChem* **2015**, *80*, 656–664.

[41] D. Awad, L. Damian, M. Winterhalter, G. Karlsson, K. Edwards, D. Gabel, *Chem. Phys. Lipids* **2009**, *157*, 78–85.

[42] V. Ďorďovič, Z. Tošner, M. Uchman, A. Zhigunov, M. Reza, J. Ruokolainen, G. Pramanik, P. Cígler, K. Kalíková, M. Gradzielski, P. Matějíček, *Langmuir* **2016**, *32*, 6713–6722.

[43] W. N. Lipscomb, A. R. Pitochelli, M. F. Hawthorne, *J. Am. Chem. Soc.* **1959**, *81*, 5833–5834.

[44] R. Hoffmann, W. N. Lipscomb, *J. Chem. Phys.* **1962**, *37*, 520–523.

[45] I. B. Sivaev, A. V. Prikaznov, D. Naoufal, *Collect. Czech. Chem. Commun.* **2010**, *75*, 1149–1199.

[46] W. H. Knoth, H. C. Miller, D. C. England, G. W. Parshall, E. L. Muetterties, *J. Am. Chem. Soc.* **1962**, *84*, 1056–1057.

[47] T. Takeuchi, V. Bagnacani, F. Sansone, S. Matile, *ChemBioChem* **2009**, *10*, 2793–2799.

[48] V. Francisco, A. Piñeiro, W. M. Nau, L. García-Río, *Chem. A Eur. J.* **2013**, *19*, 17809–17820.

[49] M. Nishihara, F. Perret, T. Takeuchi, S. Futaki, A. N. Lazar, A. W. Coleman, N. Sakai, S. Matile, *Org. Biomol. Chem.* **2005**, *3*, 1659–1669.

[50] M. Melak, M. Plessner, R. Grosse, *J. Cell Sci.* **2017**, *130*, 525–530.

[51] K. W. Teng, Y. Ishitsuka, P. Ren, Y. Youn, X. Deng, P. Ge, S. H. Lee, A. S. Belmont, P. R. Selvin, *eLife* **2016**, *5*, e20378.

[52] W. C. de Vries, D. Grill, M. Tesch, A. Ricker, H. Nüsse, J. Klingauf, A. Studer, V. Gerke, B. J. Ravoo, *Angew. Chem. Int. Ed.* **2017**, *56*, 9603–9607.

[53] J. Wehland, M. Osborn, K. Weber, *Proc. Nat. Acad. Sci.* **1977**, *74*, 5613–5617.

[54] M. An, D. Wijesinghe, O. A. Andreev, Y. K. Reshetnyak, D. M. Engelman, *Proc. Nat. Acad. Sci.* **2010**, *107*, 20246–20250.

[55] M. M. Javadpour, M. M. Juban, W.-C. J. Lo, S. M. Bishop, J. B. Alberty, S. M. Cowell, C. L. Becker, M. L. McLaughlin, *J. Med. Chem.* **1996**, *39*, 3107–3113.

[56] H. M. Ellerby, W. Arap, L. M. Ellerby, R. Kain, R. Andrusiak, G. Del Rio, S. Krajewski, C. R. Lombardo, R. Rao, E. Ruoslahti, D. E. Bredesen, R. Pasqualini, *Nat. Med.* **1999**, *5*, 1032–1038.

[57] J. Hoyer, U. Schatzschneider, M. Schulz-Siegmund, I. Neundorf, *Beilstein J. Org. Chem.* **2012**, *8*, 1788–1797.

[58] M. Acar, D. Tatini, B. W. Ninham, F. Rossi, N. Marchettini, P. Lo Nostro, *Molecules* **2022**, *27*, 8519.

[59] K. I. Assaf, B. Begaj, A. Frank, M. Nilam, A. S. Mougharbel, U. Kortz, J. Nekvinda, B. Grüner, D. Gabel, W. M. Nau, *J. Org. Chem.* **2019**, *84*, 11790–11798.
[60] M. Hou, R. Lu, A. Yu, *RSC Adv.* **2014**, *4*, 23078–23083.
[61] Y. Levin, *Phys. Rev. Lett.* **2009**, *102*, 147803.
[62] W. Kunz, P. Lo Nostro, B. W. Ninham, *Curr. Opin. Colloid Interface Sci.* **2004**, *9*, 1–18.
[63] P. Lo Nostro, B. W. Ninham, A. Lo Nostro, G. Pesavento, L. Fratoni, P. Baglioni, *Phys. Biol.* **2005**, *2*, 1.
[64] S. He, F. Biedermann, N. Vankova, L. Zhechkov, T. Heine, R. E. Hoffman, A. De Simone, T. T. Duignan, W. M. Nau, *Nat. Chem.* **2018**, *10*, 1252–1257.
[65] H. Tandon, P. Ranjan, T. Chakraborty, V. Suhag, *Mol. Diversity* **2021**, *25*, 249–262.

Manuscript received: March 1, 2024
Accepted manuscript online: May 7, 2024
Version of record online: June 14, 2024